International Journal of Advanced Research in Engineering and Related Sciences
Available online at: www.ijarers.com
Vol 1 Issue 5 (9-24)

Sustainable Treatment of Dye-Laden Wastewater via Adsorption on Phosphoric Acid-Activated Carbon from Palm-Kernel Shells

Michael Aziegbe [1], Isaac Enuma *[2], Adewumi Adegoroye [3], Zahradeen Muhammad [4], Sobur Olalekan [5], Stephen Ayankoso [6], Abraham Ajayi [7], Temitope Ademati [7]

[1] Department of Chemical Engineering, Faculty of Engineering, University of Benin, Benin city, Edo State, Nigeria.
[2] Department of Civil Engineering, Faculty of Engineering, University of Benin, Benin city, Edo State, Nigeria.
[3] Department of Chemistry, University of Ibadan, Ibadan, Oyo State, Nigeria.
[4] Department of Chemistry, King fahd University of Petroleum and Minerals, Dhahran, Saudi Arabia.
[5] Department of Microbiology, Ladoke Akintola University of Technology, Ogbomosho, Oyo State, Nigeria.
[6] Department of Agriculture, Ladoke Akintola University of Technology, Ogbomosho, Oyo State, Nigeria.
[7] Department of Chemical Sciences, Faculty of Science, Adekunle Ajasin University, Akungba Akoko, Ondo State, Nigeria.

Abstract

The purpose of this study is to examine the potentiality of palm kernel shell-derived activated carbon (PKSAC) as an economically viable and sustainable adsorbent for the elimination of methyl red dye from textile wastewater. Being one of the major contributors of water pollution via the discharge of toxic and non-biodegradable dyes, the textile sector urgently needs to adopt efficient and sustainable treatment mechanisms. This research will solve this issue by utilizing agricultural waste, i.e., palm kernel shells, to produce activated carbon, thus promoting recycling of waste and preventing environmental pollution. The research seeks to optimize the process of adsorption to achieve effective removal of dye, offering a new alternative solution to conventional treatment that is ineffective and costly. The process involves activation of palm kernel shells to produce activated carbon through carbonization and chemical activation by phosphoric acid. Adsorbent developed is analyzed through techniques such as BET analysis, SEM, and FTIR for surface area, pore structure, and functional group, respectively. Batch adsorption experiments are carried out to analyze the effect of important parameters like pH, contact time, initial dye concentration, and adsorbent dosage on methyl red dye removal efficiency. Response Surface Methodology (RSM) is used to maximize the adsorption process and to determine the optimal conditions for optimal dye removal. The results confirm that PKSAC possesses a high surface area (275.762 m^2/g) and porosity, hence a good adsorbent for dye removal. Optimal conditions for maximum dye removal efficiency (94.82%) are an adsorbent dosage of 5.05 g/L, contact time of 52.5 minutes, concentration of 300 mg/L of dye, and neutral pH of 7.0. Adsorption follows a pseudo-second-order kinetic model, which validates chemisorption as the prevailing mechanism. The study suggests the potential of PKSAC as an inexpensive, environmentally friendly alternative to industrial-activated carbons for the treatment of textile wastewater. The findings conclude that PKSAC can effectively be used in managing dye pollution, resulting in environmental conservation and green waste management. Future research should scale up the yield of PKSAC and evaluate its application towards decontamination of other toxicants.

Keywords: Palm kernel shell activated carbon, methyl red dye, textile wastewater, adsorption, phosphoric acid activation, sustainable wastewater treatment, response surface methodology, BET analysis, SEM, FTIR, pore structure, chemisorption, pseudo-second-order kinetics, dye removal efficiency

INTRODUCTION

Textile industries are one of the most important sectors of the global economy as they generate employment and contributed a great deal to the gross domestic product (GDP) of developed and developing countries. In various developing nations such as India, China, Bangladesh, and Vietnam, textile manufacturing is considered a part of industrial development, which contributes the maximum share towards export revenues. However, despite its economic importance, the textile industry has been considered one of the most important consumers of water and chemicals, with severe environmental concern. Every stage of textile production-spinning, weaving, dyeing, printing, and finishing-generates huge amounts of wastewater that contain complex mixtures of pollutants such as dyes, salts, heavy metals, and other hazardous organic and inorganic chemicals.

The textile wastewater is mainly characterized by high chemical oxygen demand (COD), biological oxygen demand (BOD), and the presence of toxic, non-biodegradable dyes. These dyes, being synthetic organic compounds, are actually designed to be highly resistant to fading when exposed to sunlight, water, and other chemicals. For this very reason, they are resistant to natural biodegradation and hence persist in the environment, decreasing the light input in bodies of water and hindering photosynthesis by aquatic life. Indeed, studies have demonstrated that untreated textile effluents may cause serious ecological effects, such as the bioaccumulation of toxic substances in aquatic organisms and the contamination of drinking water sources (Donkadokula et al., 2020).

Besides dyes, heavy metals like chromium, cadmium, lead, and copper are also commonly present in textile wastewater. These metals come from different processes, including dyeing and printing, where metal-based mordants are used to fix dyes onto fabrics. The release of heavy metals into aquatic systems poses long-term risks to both environmental and human health due to their toxicity, persistence, and tendency to bio-accumulate in living organisms (Naveenraj et al., 2021). Thus, effective treatment of textile wastewater is critical to mitigate its adverse impacts.

Starting from conventional methods, such as coagulation, flocculation, and activated sludge processes, to the newest technologies involving membrane filtration, advanced oxidation processes (AOPs), and low-cost material-based adsorption, a range of wastewater treatment techniques has been developed within the last ten years by Zhang et al. (2021). Despite this fact, most of these methods either involve excessively high treatment costs or show low efficiency in their applications on an industrial scale and thus call for the development of more viable and affordable technologies. The rapid growth of the textile industry is resulting in higher volumes of wastewater being discharged into natural water bodies without adequate treatment. Textile effluents contain high concentrations of complex pollutants, including synthetic dyes and heavy metals, which are resistant to conventional biological degradation processes. Thus, untreated or partially treated wastewater can cause serious environmental problems, such as water pollution, soil contamination, and harm to aquatic ecosystems.

Existing wastewater treatment methods face several challenges. Conventional methods, such as coagulation-flocculation and activated sludge processes, often fail to completely remove colour and toxic substances from textile wastewater. Moreover, these methods generate large volumes of sludge, which requires further treatment and disposal, adding to operational costs and environmental burden (Hynes et al., 2020). The advanced techniques of membrane filtration and advanced oxidation processes (AOPs) are mostly unaffordable by small and medium-sized enterprises (SMEs) and show higher removal efficiencies. There is, therefore, an urgent need for the development of inexpensive and high-efficiency treatment technologies for efficiently removing dyes, heavy metals, and other pollutants in wastewater generated from textile industries. The present study has attempted to fill these gaps by exploring innovative approaches that may prove viable economically and environmentally sustainable.

MATERIALS AND METHOD

A. CHEMICAL AND REAGENTS

All chemicals and reagents used in this work were of analytical grade used without further purification. The majority of them were purchased from a laboratory materials vendor in Benin city. Edo state. The details of each reagent, their sources and what they were used for in this work are summarized below in Table 1

S/N	Chemicals/Reagents	Manufacturer	Uses
1	Phosphoric acid (H_3PO_4)	Guangdong Guanghua Sci-Tech C0., Ltd.	For activating the carbonized palm kernel shell
2	Potassium hydroxide (KOH)	Trust Chemical Laboratories	For adjusting the pH of the wastewater
3	Hydrochloric acid (HCl)	Loba Chemie Pvt. Ltd	For adjusting the pH of the wastewater sample
4	Methyl red dye	Trust Chemical Laboratories	For testing the capability of the adsorbent
5	Deionized Water	Luco chemicals	Used for washing and dilution purposes

B. PREPARATION OF PALM KERNEL SHELLS ACTIVATED CARBON

Palm kernel shell was collected from a local palm oil mill in Edo State, Nigeria. Dirt and residual flesh were removed and then the PKS was thoroughly washed with deionized water, to remove surface impurities such as dust particles and ions that would cause variations in the results of the experiments. The washed shells were then dried at 105°C for three hours in an oven to eliminate moisture content. Once dried, the shells were crushed. The carbonization process was carried out by heating the crushed PKS in a muffle furnace at 650°C for two hours under a limited oxygen supply. After carbonization, the material was allowed to cool to room temperature before undergoing chemical activation. Chemical activation was performed using a 30% phosphoric acid (H_3PO_4) solution. The carbonized PKS was impregnated with the acid by continuous stirring for two hours, followed by a soaking period of twelve hours to ensure thorough penetration of the acid into the carbon structure. Following the activation process, the adsorbent was washed with distilled water until a neutral pH was achieved. The washed activated carbon was then dried at 110°C for six hours before being stored in an airtight container for subsequent experimental use.

C. CHARACTERIZATION OF ACTIVATED CARBON SAMPLE

The adsorbent underwent characterization prior to the adsorption process. Various properties of the adsorbent were assessed using different techniques:

i. BET Method (JW-DA, 76502057en): This method was employed to determine the specific surface area, pore size distribution, pore volume, total pore volume, and pore volume distribution of the adsorbent.
ii. SEM (JEOL JSM-7600F): Scanning Electron Microscopy was utilized to examine the surface morphology of the adsorbent.
iii. FTIR (Nicolet iS10 FT-IR Spectrometer): Fourier-Transform Infrared Spectroscopy was used to irradiate the sample and identify the active functional groups present on the surface of the adsorbent.
iv. XRD (Rigaku D/Max-IIIC X-ray Diffractometer): X-ray Diffraction analysis was performed to determine the crystallinity of the activated carbon. These characterization techniques provide valuable insights into the physical and chemical properties of the adsorbent, helping to understand its suitability and performance for adsorption purposes.

D. BATCH ADSORPTION EXPERIMENT

Preparation of Dye Solution:

A stock solution of 1000 mg/L methyl red dye was prepared and diluted as required.

ADSORPTION STUDIES:

The batch adsorption experiments were conducted using separate 250ml conical flasks, with each flask containing 100 ml of waste water. Various amounts of the PKS-AC were added to the waste water samples, ranging from 0.1 to 10.0 g/L. The contact time for each experiment ranged from 15 to 90 minutes. These experiments were carried out within a pH range of 5 to 9, as outlined in the experimental design. To facilitate mixing of the waste water with the PKS-AC adsorbent, the glass conical flasks were positioned on an orbital shaker machine set at an rpm speed of 150 for the specified contact time. After adsorption, the solutions were filtered, and a 10ml sample was extracted from each suspension for further analysis or assessment, using a UV- Vis spectrophotometer at the maximum wavelength (λ_max = 540 nm).

Determination of Removal Efficiency:

The amount of dye adsorbed at equilibrium (Ω, mg/g) and the dye removal efficiency was calculated using:

$$q_e = \frac{(C_o - C_e)V}{W} \text{ ---------- (3.1)}$$

$$R = \frac{C_o - C_f}{C_o} \times 100 \text{ ----------(3.2)}$$ where:

Where q is the amount of metal ion adsorbed by the adsorbent (mg/g); C_o is the initial dye concentration in contact with the adsorbent (mg/L), C_e is the equilibrium dye concentration (mg/L), C_f is the dye concentration after the batch adsorption, V is the volume of aqueous solution put in contact with the adsorbent in liters (L) and m is the adsorbent dosage in grams (g).

E. RESPONSE SURFACE OPTIMIZATION OF DYE REMOVAL (Design of Experiment)

In the study, a Response Surface Methodology (RSM) model was developed and employed to optimize the adsorption process for waste water. The optimization process was carried out with the assistance of RSM, utilizing Central Composite Design (CCD provided by the Design Expert program (version 13, Stat-Ease Inc., Minneapolis, USA**).** A Central Composite Design (CCD) **is** a widely used experimental design for Response Surface Methodology (RSM)**,** which helps in optimizing processes and understanding interactions between variables. CCD is particularly useful for building second-order (quadratic) models and exploring the effects of multiple independent variables on a response variable. The factors considered were:

i. Adsorbent Dosage (g/L): 0.1 – 10.0 g/L
ii. Contact Time (min): 15 – 90 min
iii. Initial Concentration (mg/L): 100 – 500 mg/L
iv. pH: 5 – 9

The Central Composite Design generated a total of 30 runs to optimize these four factors. These factors encompassed adsorbent dosages ranging from 0.1 to 10 g/L, a pH range of 5 to 9, initial concentration ranging from 100 to 500 mg/L and contact times spanning from 15 to 90 minutes. The primary objective of these experiments was to optimize the removal of dyes from waste water using the composite adsorbent.

RESPONSE SURFACE METHODOLOGY(RSM) OPTIMIZATION

Table 2: Build information

Build	Information
File Version	13.0.1.0
Study Type	Response Surface
Design Type	Central Composite
Design Model	Quadratic
Build Time (ms)	1.0000
Subtype	Randomized
Runs	30.00
Blocks	No Blocks

Table 3: Design Factors

Name	Minimum	Maximum	Coded Low	Coded High	Mean	Std. Dev.
A: Adsorbent dosage (g/L)	0.1000	10.00	-1 ↔ 2.58	+1 ↔ 7.53	5.05	2.25
B: Contact Time (minute)	15.00	90.00	-1 ↔ 33.75	+1 ↔ 71.25	52.50	17.06
C: Dye conc. (mg/L)	100.00	500.00	-1 ↔ 200.00	+1 ↔ 400.00	300.00	90.97
D: pH	5.00	9.00	-1 ↔ 6.00	+1 ↔ 8.00	7.00	0.9097

Table 4: Experimental runs generated by design expert

Std	Run	Factor 1 A: Adsorbent dosage g/L	Factor 2 B: Contact Time minutes	Factor 3 C: Dye conc. mg/L	Factor 4 D: pH	Dye removal (%) Conc. mg/L
12	1	7.525	71.25	200	8	
6	2	7.525	33.75	400	6	
4	3	7.525	71.25	200	6	
27	4	5.05	52.5	300	7	
13	5	2.575	33.75	400	8	
23	6	5.05	52.5	300	5	
7	7	2.575	71.25	400	6	
29	8	5.05	52.5	300	7	
24	9	5.05	52.5	300	9	
5	10	2.575	33.75	400	6	
9	11	2.575	33.75	200	8	
20	12	5.05	90	300	7	
2	13	7.525	33.75	200	6	
21	14	5.05	52.5	100	7	

14	15	7.525	33.75	400	8	
8	16	7.525	71.25	400	6	
25	17	5.05	52.5	300	7	
16	18	7.525	71.25	400	8	
19	19	5.05	15	300	7	
28	20	5.05	52.5	300	7	
22	21	5.05	52.5	500	7	
30	22	5.05	52.5	300	7	
1	23	2.575	33.75	200	6	
3	24	2.575	71.25	200	6	
15	25	2.575	71.25	400	8	
18	26	10	52.5	300	7	
10	27	7.525	33.75	200	8	
26	28	5.05	52.5	300	7	
11	29	2.575	71.25	200	8	
17	30	0.1	52.5	300	7	

RESULTS

A. PALM KERNEL-SHELL ACTIVATED CARBON CHARACTERIZATION

The activated carbon consisting of palm kernel-shell, was subjected to the Brunauer-Emmett-Teller (BET) Scanning Electron Microscopy method. The BET method provided information on pore size distribution which influenced the accessibility of the PKSAC sites for different sized molecules. Also, the SEM provided a high-resolution image of the activated carbon's surface morphology. Also, the SEm micrographs visually confirmed the development of a porous network within the activated carbon.

The BET analysis provided insights into the porous structure and adsorption properties of the adsorbent, which is critical for evaluating its efficiency in dye removal as seen in Table 5

Table 5: Summary of the BET analysis on the activated carbon (Palm kernel-shell)

Method	**Surface Area(m^2/g)**	**Pore volume (cc/g)**	**Pore Diameter (nm)**	**Adsorption Energy (kJ/mol)**
Multi-point BET	275.762	-	-	-
Langmuir	464.380	-	-	-
DR	393.400	0.140	3.866	6.725
BJH	278.755	0.135	2.108	-
DA	-	0.195	2.140e+00	1.832

The Multi-point BET method was applied to measure the specific surface area of the adsorbent. The resulting BET surface area was calculated to be approximately 275.762 m^2/g. This value indicates the extent of surface available for adsorption, which is essential for evaluating the adsorbent's capacity to remove methyl red from dye wastewater. The Langmuir method was also to characterize the adsorbent. This method is based on the assumption of a monolayer coverage of adsorbate molecules on the adsorbent surface. From the Langmuir data the surface area of the adsorbent was also calculated, with a value of 464.380 m^2/g corroborating the BET surface area findings. The Langmuir adsorption isotherm model's correlation coefficient $r^2 = 0.988$ indicates a relatively strong fit, supporting the monolayer adsorption assumption for this adsorbent material. The DA method was employed to further examine microporosity within the adsorbent. The DA analysis provided a micropore volume of 0.195 cc/g and an average pore diameter (mode) of 2.14 nm. These values suggest a predominantly microporous structure suitable for adsorbing small molecules.

The energy of adsorption (Best E) was calculated to be 1.832 kj/mol, which gives insight into the strength of interaction between the adsorbent and adsorbate. Also using the DR method, additional information on microporosity was gathered yielding a micropore surface area of 393.400 m^2/g. The adsorption energy 6.725 kj/mol, points to physical adsorption rather than chemical bonding, aligning with the general characteristics of activated carbon. The average pore width from the DR was noted to be 3.866 nm. To analyse the mesoporous structure, the Barrett-joyner-Halcnda (BJH) method was

applied using the nitrogen adsorption data. The BJH adsorption cumulative pore volume was found to be 0.135 cc/g, and the average pore diameter for the mesopores was calculated at 2.108 nm. The cumulative pore volume and pore size distribution derived from the BJH method show the presence of mesopores in addition to micropores further enhancing the material's ability to adsorb dyes effectively due to combined effect of both pores' types.

The SEM images below, provides a detailed view of the surface morphology of the adsorbent, specifically showing the porous structure, rough surface, and potential microporous or mesoporous cavities on the palm kernel-shell activated carbon. The rough texture and visible pores enhance surface area of the adsorbent, contribute to more active site for adsorption. This high surface area aligns with BET analysis obtained (275.762 m^2/g) supporting efficient adsorption of dyes (methyl red) from dye wastewater. The DA and BJH analysis, showing micropore volume and pore size distribution, indicates the presence of micropores and mesopores, which are crucial for capturing small and larger dye concentration respectively. The SEM images corroborate these findings, visually suggesting the adsorbent's capability to adsorb dyes of different concentration. The pore structure in the SEM images provides the surface heterogeneity required for models like Freundlich, while the possibility of monolayer adsorption aligns with the Langmuir model.

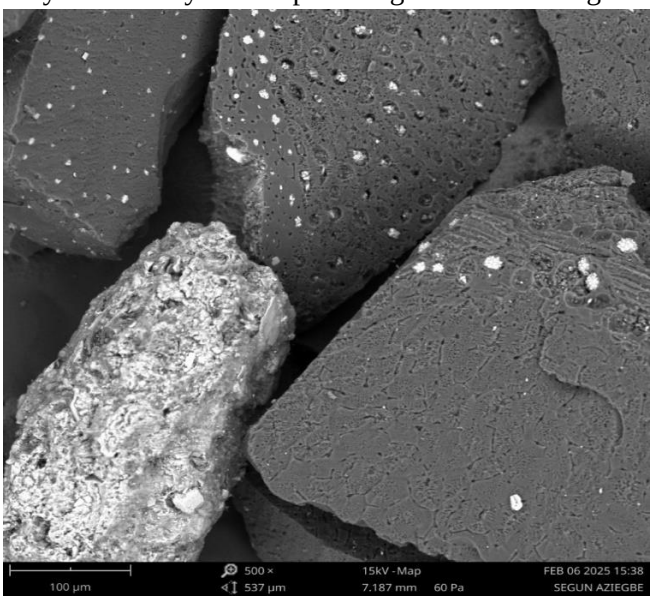

Figure 1: Surface Morphology of Palm kernel-shell Activated carbon at 500x Magnification.

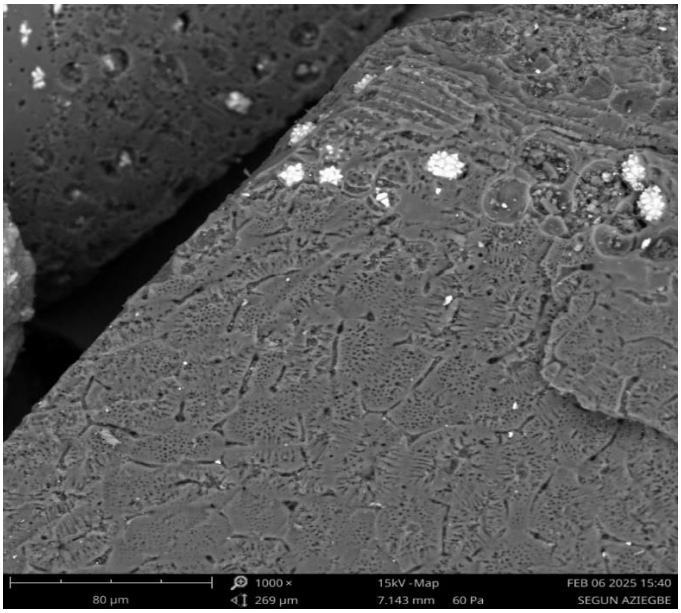

Figure 2: Surface Morphology of Palm kernel-shell Activated Carbon at 1000x Magnification

Figure 1 highlights the microstructure of the adsorbent, revealing a rough surface with visible micropores and irregular textures that contribute to increased adsorption site. While Figure 2 captures the broader surface features, including larger pore formations providing insight into the adsorbent's capacity to adsorb dyes efficiently.

B. FOURIER TRANSFORM INFRARED SPECTROSCOPY (FTIR)

FTIR analysis was performed to identify the functional groups present on the surface of the activated carbon, which play a significant role in adsorption processes. The analysis of the FTIR spectrum helps in identifying key chemical bonds and interactions, which are critical in understanding the adsorption affinity of adsorbent in dye wastewater. The FTIR spectrum provided in figure 3 shows a series of peaks at specific wavenumbers (cm^{-1}), each corresponding to the vibration of a particular chemical bond.

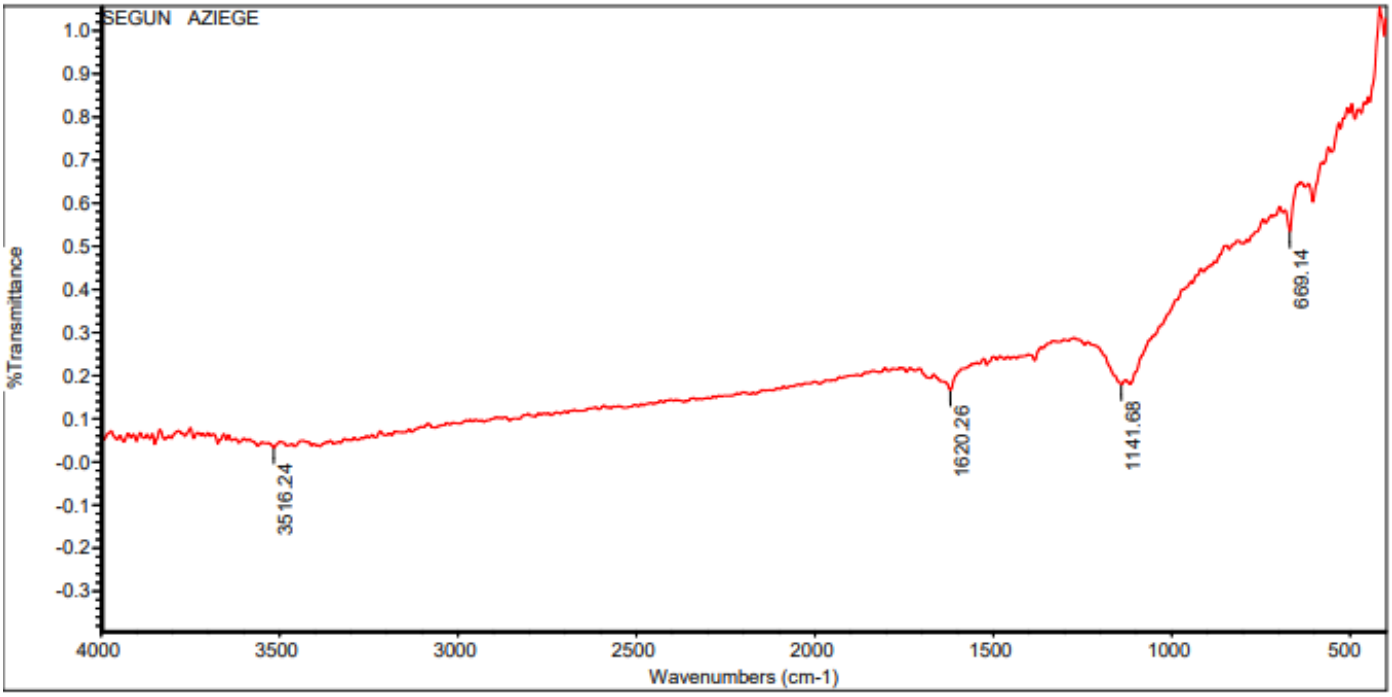

Figure 3: Fourier Transform Infrared Spectroscopy (FTIR) Analysis of PKSAC

Table 6: Summary of Spectrum Peaks for PKSAC

Peak Number	Position (cm^{-1})	Intensity	Functional Groups	Comment
1	669.14	0.534	C-H Bending (Aromatic)	Typically associated with aromatic out-of-plane bending vibrations, indicating the presence of benzene-like structures.
2	1141.68	0.179	C-O Stretch (Alcohols, Esters)	Suggests the presence of ether or ester functional groups, commonly found in organic molecules.
3	1620.26	0.166	C=C Stretch (Alkenes, Aromatics)	This peak corresponds to the stretching vibrations of C=C bonds, indicating unsaturated compounds or aromatic rings.
4	3516.24	0.0328	O-H Stretch (Alcohols, Phenols)	Represents the presence of hydroxyl (-OH) groups, which could be from alcohols, phenols, or adsorbed moisture.

Table 6 summarizes FTIR analysis of the adsorbent that detects the presence of the main functional groups that are liable for its adsorptive nature.

The highest peak at 669.14 cm^{-1}, which is the area where out-of-plane bending vibrations of C-H bonds in aromatic systems take place. Its appearance indicates that the activated carbon contains aromatic structures that are an important component of its carbon structure. Aromatic rings are highly stable and contribute to the structural strength of the material, thus can be utilized in adsorption operations for non-polar substances. This peak is conclusive evidence that the carbon derived from palm kernel shells still retains its organic aromatic character despite going through the activation process.

At peak 1141.69 cm^{-1}, this region is due to C-O stretching vibrations, which are typical of oxygen-functional groups such as ethers, alcohols, or esters. The presence of this peak confirms that the surface of the activated carbon consists of oxygenated functional groups. These groups are likely introduced during activation or are present as native groups in the palm kernel shell precursor. The occurrence of C-O bonds enhances the hydrophilicity of the material, and as such, it is more effective in the adsorption of polar compounds, such as water or oxygen-containing organic molecules. This is particularly important in the applications of water purification wherein adsorbent-polar contaminant interaction is relevant. 1620.26 cm^{-1} is the second distinguishing feature of the spectrum. This peak occurs from C=C stretching vibrations from conjugated systems or aromatic rings and is yet another sign of aromatic structures within the activated carbon. This part of the spectrum will also have overlapped O-H bending vibrations that point to adsorbed water or hydroxyl groups at the surface of the activated carbon. The presence of these groups will impact the material's adsorption properties, particularly for polar or ionic adsorbates. This peak, therefore, not only substantiates the aromatic nature of the carbon but also proposes the probable presence of surface hydroxyl groups, which will increase the material's interaction with polar adsorbents.

Finally, the 3516.24 cm^{-1} peak is also indicative of the O-H stretching vibrations, typical for hydroxyl groups (-OH) or water molecules. This peak indicating that there are hydroxyl groups, which are water-loving in nature, on the activated carbon surface. Hydroxyl groups can enhance the ability of the material to adsorb water and polar compounds. The relatively low intensity of this peak means that hydroxyl groups are in moderate concentrations, typical for activated carbon materials. The occurrence of these groups is particularly important for applications where adsorption of polar or hydrophilic compounds is required, e.g., in heavy metal or organic pollutant removal from water.

C. MODEL FITTING (Response Surface Methodology)

FIT STATISTICS

Table 7: Fit Statistics

R^2	**0.9666**
Adjusted R^2	0.9355
Predicted R^2	0.8275
Adeq Precision	16.6925
Std. Dev.	6.24
Mean	57.64
C.V. %	10.82

The **Predicted R^2** of 0.8275 is in reasonable agreement with the **Adjusted R^2** of 0.9355; i.e., the difference is less than 0.2. The fit statistics table indicates the model performance to estimate methyl red removal efficiency. The coefficient of determination (R^2) is 0.9666, indicating that the model accounts for 96.66% of the variation in the response, which is a good fit. The adjusted R^2 of 0.9355 corrects for the number of predictors and sample size such that the model is stable and not over fitted. The estimated R^2 of 0.8275 shows that the model has considerable predictive ability, though a little lower than the adjusted R^2, and is possibly indicative of some room for improvement. The adequate precision of 16.6925 is well in excess of the threshold of 4, further confirming that the model has very high signal-to-noise ratio and is stable for design space search. A standard deviation of 6.24 indicates the range of variability in the residuals, with the mean response being 57.64. The coefficient variation (C.V.%) of 10.82% represents the range of variability in terms of the mean and indicates an optimal range of accuracy for the model prediction.

Final Equation in Terms of Coded Factors

$$\boldsymbol{Dye\ Removal}\ (\%) = \mathbf{94.82 + 10.77A + 7.60B + 5.44C - 2.75D + 4.50AB + 0.9133AC - 2.38AD + 1.44BC - 1.56BD + 5.97CD - 13.02A^2 - 11.15B^2 - 13.37C^2 - 8.94D^2}$$

The equation in terms of coded factors can be used to make predictions about the response for given levels of each factor. By default, the high levels of the factors are coded as +1 and the low levels are coded as -1. The coded equation is useful for identifying the relative impact of the factors by comparing the factor coefficients.

D. ANOVA-BASED STATISTICAL EVALUATION OF METHYL RED REMOVAL EFFICIENCY

ANOVA for Quadratic model

Response 1: Dye Removal

Table 8: Response 1: Dye Removal

Source	Sum of Squares	df	Mean Square	F-value	p-value	
Model	16904.89	14	1207.49	31.02	< 0.0001	significant
A-Adsorbent dosage	2785.74	1	2785.74	71.57	< 0.0001	
B-Contact Time	1387.88	1	1387.88	35.66	< 0.0001	
C-Dye conc.	709.93	1	709.93	18.24	0.0007	
D-pH	182.06	1	182.06	4.68	0.0471	
AB	324.24	1	324.24	8.33	0.0113	
AC	13.34	1	13.34	0.3429	0.5669	
AD	90.35	1	90.35	2.32	0.1484	
BC	32.98	1	32.98	0.8472	0.3719	
BD	38.92	1	38.92	1.00	0.3332	
CD	569.52	1	569.52	14.63	0.0017	
A^2	4651.67	1	4651.67	119.51	< 0.0001	
B^2	3412.70	1	3412.70	87.68	< 0.0001	
C^2	4902.90	1	4902.90	125.97	< 0.0001	
D^2	2190.78	1	2190.78	56.29	< 0.0001	
Residual	583.83	15	38.92			
Lack of Fit	503.71	10	50.37	3.14	0.1090	not significant
Pure Error	80.12	5	16.02			
Cor Total	17488.72	29				

The Model F-value of 31.02 implies the model is significant. There is only a 0.01% chance that an F-value this large could occur due to noise. In the table, the whole model is highly significant with a p-value of less than 0.0001, so it can be concluded that the selected factors taken together have a significant role to play in methyl red removal efficiency. Among the individual factors, the effect is significant for adsorbent dosage, contact time, dye concentration, and pH but less significant for pH compared to the others. Statistically significant are the interactions such as that between contact time and adsorbent dosage (AB) and between dye concentration and pH (CD), which indicate that these pairs of factors have effects on the adsorption process. Others, such as AC, AD, BC, and BD, are revealed to be non-significant and therefore reflect their combined effect not to be significantly changing the response. All the quadratic terms A^2, B^2, C^2, and D^2 are very high, indicating that the interaction between the factors and the response is quadratic rather than linear. This means that methyl red removal efficiency is a function of nonlinear effects of the input variables.

The residual term explains unexplained variation in the model, and the lack of fit decides whether the model is a good fit for observed data or not. The lack of fit has a p-value of 0.1090, which means that it is not significant, and hence the model provides a good fit to the experimental data. There is a 10.90% chance that a Lack of Fit F-value this large could occur due to noise.

Overall, the analysis confirms that the selected factors play a significant role in the adsorption process, with some interactions playing an important role. The presence of significant quadratic terms implies that optimization of the adsorption conditions should consider nonlinear effects in order to achieve the maximum methyl red removal efficiency.

E. INTERACTION OF INDEPENDENT VARIABLES ON METHYL RED REMOVAL

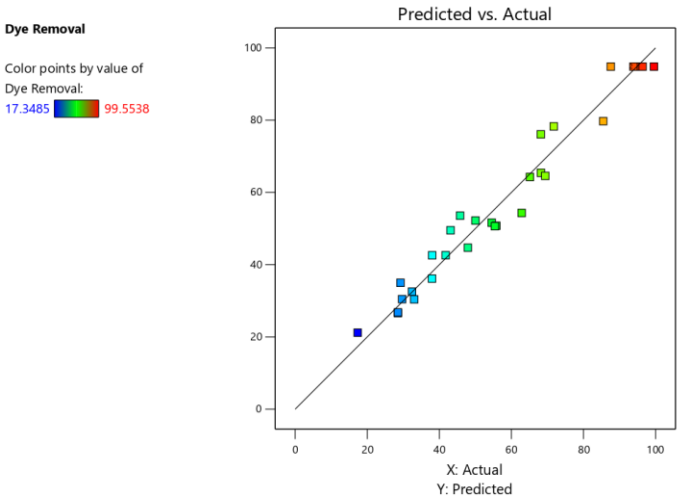

Figure 4:Predicted vs Actual graph on dye removal efficiency

Figure 4 graph shows a scatter plot of actual vs predicted values of dye removal and displays the accuracy of the model. Actual values are plotted on the x-axis and predicted values on the y-axis. A diagonal reference line shows the ideal case where predicted values are equal to actual values. Each point is shaded according to the degree of removal of dye, on a scale ranging from blue (lower removal values of around 17.35%) to red (greater removal values of close to 99.55%). Points falling on the line of perfect correlation are points at which the prediction by the model for the efficiency of dye removal is satisfactory. The closer the points are to this line, the closer is the agreement between prediction and reality, disagreement being represented by deviation from the line. The data points' colour gradient shows how the range of dye removal is spread across values. That both the red and blue points are dispersed along the diagonal is a good sign that the model is still accurate for the whole percentage of dye removal range. The validity of the model used for this dye removal prediction is clearly depicted in this graph, and good agreement between experimental and predicted values can be seen.

Effect of Contact Time and Adsorbent Dosage

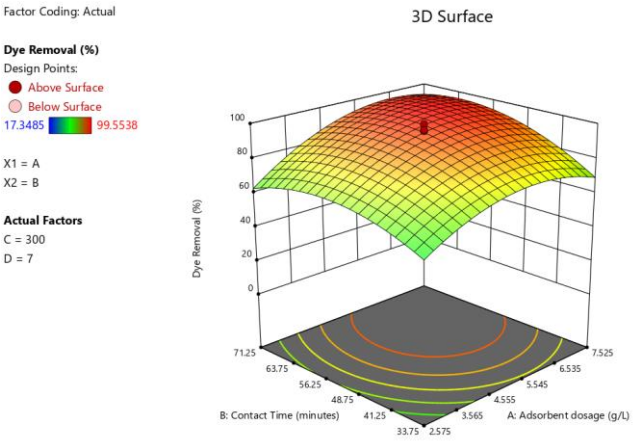

Figure 5: 3D Surface Plot for the effect of Contact time and Adsorbent Dosage

The 3D surface plot presents the interaction between contact time, adsorbent dosage, and dye removal efficiency. The x-axis represents the adsorbent dosage (g/L), and the y-axis represents the contact time (minutes). The z-axis, which is shown using the height of the surface and the color gradient, is the percentage removal of the dye. The surface is curved. It is highest for removal of dye in the red region and falls off in the green and blue regions, which indicate lower removal rates. The color graduates from green (indicating the lowest removal values) to yellow, orange, and then red at the top, which signifies the highest dye removal efficiency. The bottom contour plot gives the top view of the surface and supports the trend seen in the 3D image. From the plot, it is seen that contact time and adsorbent amount contribute significantly to the effectiveness of the removal of the dye. The factors initially contribute to the removal, as supported

by the increasing surface towards the red area. But after a certain point, the efficiency plateaus and hits a maximum. This would mean that increasing contact time or adsorbent dose may not lead to much enhancement. This graph pictorially represents the optimum conditions for maximum dye removal, in addition to showing that after a point there are decreasing returns.

Effect of Dye Concentration and Adsorbent Dosage

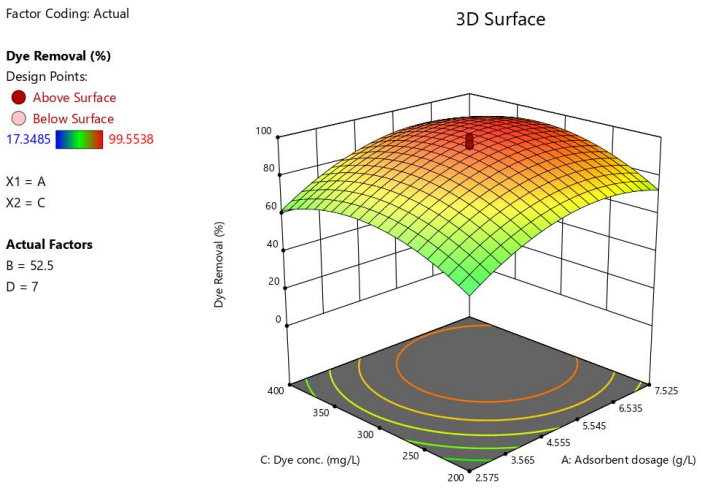

Figure 6: 3D Surface Plot for the effect of Dye concentration and Adsorbent dosage on percentage removal of Methyl Red

The design helps in finding the optimal dosage of adsorbent and concentration of dye that will give maximum removal of the dye. For example, maximum dye removal efficiency (99.5538%) is achieved at a specific point on the surface plot, which is a specific dosage of adsorbent and concentration of dye. With the increase of adsorbent dosage, the efficiency of dye removal increases but up to a point only. Once that point is reached, adding more adsorbent will make little difference to the removal of the dye, and may actually lower efficiency since it will be saturated or otherwise. With low concentrations of dye, the dye removal efficiency could be optimal since little dye needs to be removed, and the adsorbent can easily capture it. With high dye concentrations, efficiency in dye removal can be lowered by adsorbent saturation and failure to adsorb all the dye molecules. The plot demonstrates the impact of interaction between adsorbent dosage and dye concentration on dye removal. For example, with a specific dosage of adsorbent, a higher concentration of dye could lead to a drop in efficiency, while with a different dosage, the same increase would have a less significant effect.

Effect of pH and Adsorbent Dosage

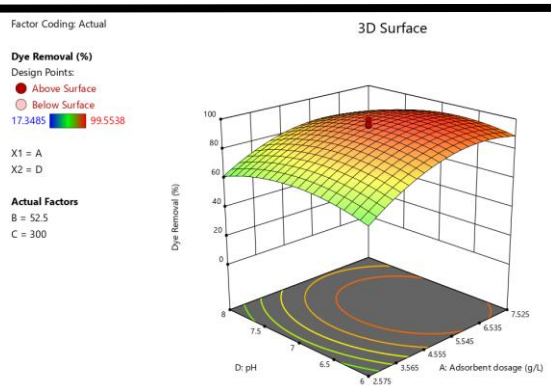

Figure 7: 3D Surface Plot for the effect of pH and Adsorbent dosage on percentage removal of Methyl Red

With increasing dosage of adsorbent, the removal efficiency of dye is significantly improved. This is evident from red and yellow spots at higher dosages of adsorbent, representing high percentages of dye removal (~100%). Increased removal of dye decreases at extremely high dosages of adsorbent, reflecting a plateau region where more adsorbent does not provide much increased removal of dye. Removal of dye is less at extremely low or high pH levels. Maximum dye removal percentages occur at intermediate pH values (around 6–7). This implies that the adsorbent effectiveness is dependent on the capacity to maintain an optimal pH level.

Effect of Dye Concentration and Contact Time

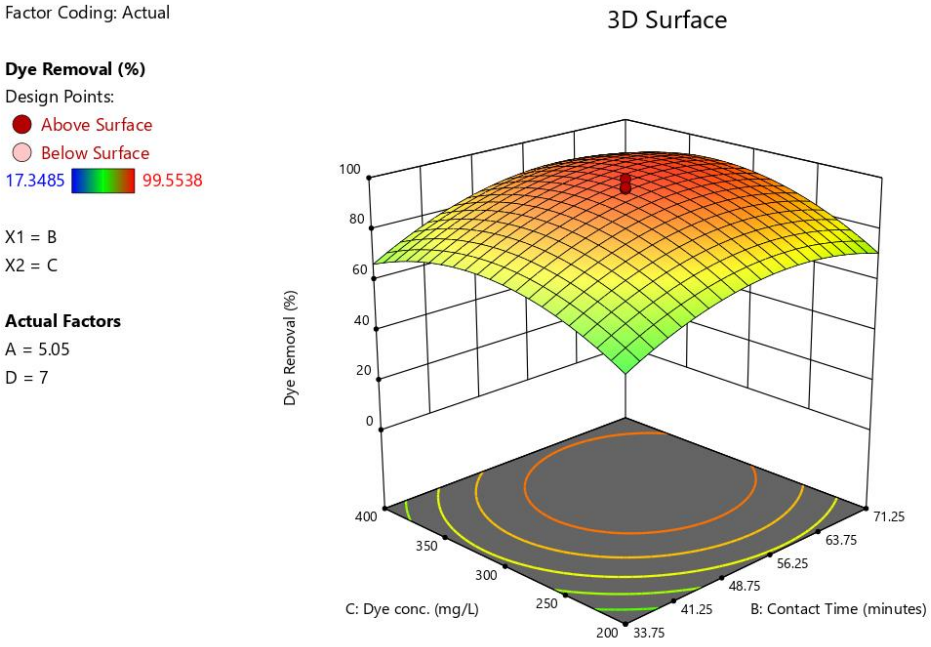

Figure 8: 3D Surface Plot for the effect of Dye concentration and Contact time on percentage removal of Methyl Red

More contact time increases the effectiveness of removal of dye. Surface is larger (yellow to red) with longer contact times, indicating maximum removal of dye (~100%). However, there is a point of saturation indicated by the trend, where further increase in contact time after some point does not yield much extra removal. Higher initial concentrations of dyes result in lower removal percentages of dyes. This is well indicated by the decrease in surface slope with higher dye concentrations, especially at low contact times. The adsorption is less efficient at higher concentrations of dye, perhaps due to saturation of the available adsorption sites. At longer contact times and with low dye concentrations, maximum dye removal. The surface is concave, i.e., favourable conditions for dye removal are moderate-to-low levels of dye concentrations and sufficient contact time. The contour plot confirms this trend, as there is a higher concentration of the contour lines at low levels of dye concentrations, i.e., steeper slopes in removal efficiency.

Effect of pH and Contact Time

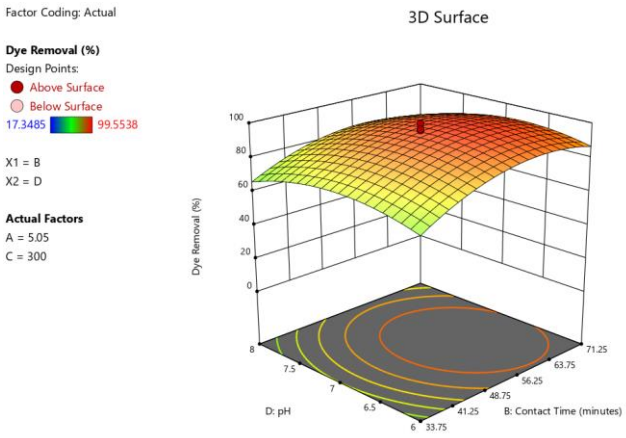

Figure 8: 3D Surface plot for the effect of pH and Contact time on percentage removal of Methyl Red

Increased contact time has the effect of enhancing dye removal, but only to a point. The surface of the graph curves, and the effect of contact time is therefore not linear. The optimal contact time appears to be some place in the middle of what we experimented with. After that optimum, higher contact time has diminishing returns, and possibly even diminishing dye removal. Visual estimation of this optimum range seems to be 50-65 minutes. At extremely low contact times (33.75 to 45 minutes), the dye removal is very low, regardless of pH. Similar to contact time, pH also possesses an optimum range. Optimum removal of dye occurs around a pH value of 7 to 7.5. Avoiding this optimum pH (either acidic towards 6 or basic towards 8) provides lower percentages of dye removal. The effect of pH seems more significant at longer contact-times. The peak (red area) on the surface is at the conditions that provide maximum dye removal. This occurs at around 50-65 minutes of contact time and pH 7 to 7.5.

Effect of pH and Dye Concentration

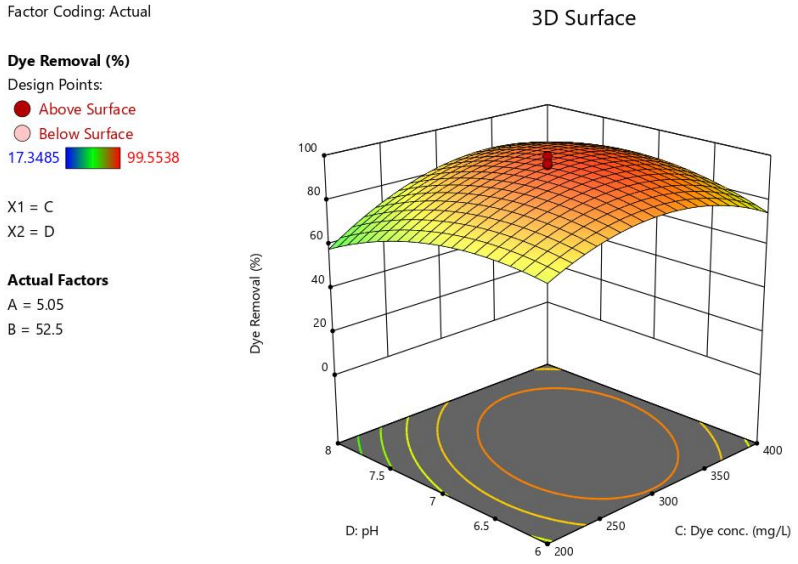

Figure 9: 3D Surface Plot for the effect of pH and Dye concentration on percentage removal of Methyl Red

Greater removal efficiency of the dye occurs at intermediate pH and low concentration of the dye. Efficiency is less at extreme low pH or high concentration of the dye. Greater efficiency of removal of the dye occurs at near neutral to slightly alkaline pH (around 6.5-7.5). Efficiency is less at very low (acidic) or very high (alkaline) pH values. This would suggest that the removal mechanism would be pH-dependent, such as variations in charge interactions, active sites, or

chemical reaction. Efficiency declines with increasing dye concentration, most likely due to saturation or a lack of sites for adsorption. There is more removal efficiency at lower dye concentrations (closer to 200 mg/L). Higher concentration of dye (up to 400 mg/L) results in reduced efficiency, possibly due to saturation effects where the removal medium (adsorbent or chemical treatment) is saturated and less effective. The 3D graph indicates that moderate pH and lower concentration of dye are ideal for effective dye removal. Higher pH levels and higher concentrations of dye reduce efficiency, and this is information which can be used to optimize wastewater treatment processes.

F. OPTIMIZATION OF THE MODEL DESIGN

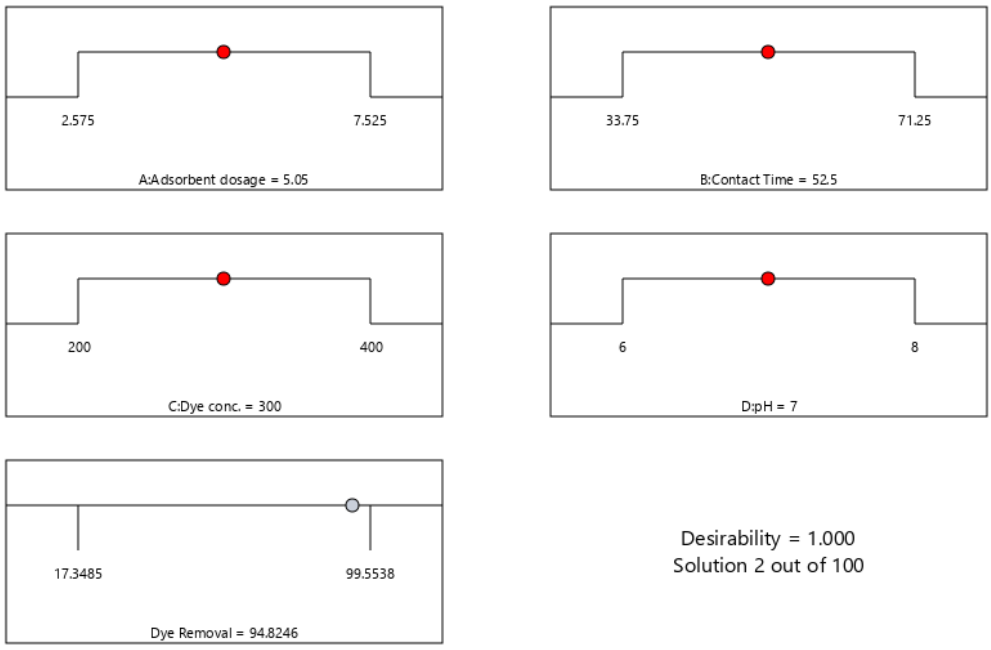

Figure 10: Optimization plot for dye removal efficiency showing the effect of Adsorbent dosage, Contact time, Dye conc., and pH.

Each subplot explains one parameter and its range (min to max values) along with the chosen optimum point. Efficiency of Dye Removal: The efficiency obtained after the last process is 94.82%, which is a very high value. The value of desirability = 1.000 indicates that the chosen set of parameters provides the optimum solution, i.e., the optimization model developed an optimum one. Solution 2 of 100, sets out some of the possible parameter combinations that were tried, and this is one of the best solutions. Adsorbent Dosage (5.05 g) is the proper adsorbent needed for optimal dye removal, but additional dosage is unlikely to be useful. Contact Time (52.5 min) offers enough interaction time for dye adsorption or elimination. Dye Concentration (300 mg/L) a medium range is optimal for efficient removal without overloading adsorptive capacity. pH (7.0), a neutral pH, seems to be best for the removal of the dye. The above figure shows the optimum set of parameters for maximum dye removal efficiency of (94.82%). The 1.000 desirability confirms that these sets of parameters are optimal for the process.

CONCLUSION

The findings of this groundwater quality assessment in Ute Community, Ikpoba Okha L.G.A., Edo State, present a concerning picture of the current state of borehole water resources relied upon by the local population. Through rigorous physicochemical and bacteriological analysis of twelve borehole samples, this study has identified multiple parameters that exceed established safety thresholds, posing significant risks to public health. The results demonstrate that while some indicators like total dissolved solids and turbidity fall within acceptable limits, critical contaminants reveal systemic challenges in water quality management. The persistent acidity of the groundwater, with pH levels ranging from 5.98 to 6.41 across most samples, creates an environment conducive to metal leaching and pipe corrosion, while simultaneously indicating inadequate natural buffering capacity of the local aquifer system of particular concern are the elevated cadmium concentrations found throughout the study area, ranging from 0.06 to 0.61 mg/L, which dramatically surpass the WHO permissible limit of 0.003 mg/L. This heavy metal contamination represents a severe long-term health hazard, as cadmium bioaccumulates in the human body and can lead to renal dysfunction, bone demineralization, and other chronic conditions even at low exposure levels. The widespread nitrate pollution, with concentrations between 30.55 and 65.85 mg/L in most samples, similarly points to substantial anthropogenic influence, likely stemming from agricultural runoff and inadequate waste disposal practices in the community. These chemical contaminants combine with microbiological threats, as evidenced by the consistent presence of fecal coliforms and E. coli, to create a multifaceted water quality crisis that demands immediate and coordinated intervention. The shallow depth of the aquifer system (2.75-6.0 meters) significantly contributes to its vulnerability, allowing surface pollutants relatively direct access to groundwater reserves. This hydrogeological characteristic, coupled with the community's reliance on on-site sanitation systems and intensive agricultural activities, creates ideal conditions for groundwater contamination. The study's findings align with broader regional patterns of groundwater quality degradation observed in Nigeria's sedimentary basins, but the specific contaminant profile in Ute Community reveals unique local challenges that require tailored solutions. The coexistence of geogenic factors (like natural aquifer acidity) and anthropogenic pressures (including poor waste management and agricultural intensification) creates a complex water quality scenario that standard treatment approaches may not adequately address. Addressing these challenges will require a multipronged strategy that combines immediate technical solutions with long-term institutional and community-based approaches. At the household level, point-of-use treatment technologies such as ceramic filters or solar disinfection systems could provide interim protection, while community-scale solutions might include the construction of centralized treatment facilities equipped to handle heavy metal removal. Regulatory enforcement must be strengthened to control pollution sources, particularly from agricultural activities and waste disposal sites. Simultaneously, community education programs are essential to build awareness about proper sanitation practices and the health risks associated with contaminated water.

Looking forward, this study highlights several critical areas for further research. Detailed contaminant source tracking through isotopic analysis could help distinguish between various pollution origins, while hydrogeological modeling would improve understanding of contaminant transport mechanisms in the local aquifer system. Evaluation of nature-based treatment solutions, such as constructed wetlands tailored to local conditions, could offer sustainable alternatives to conventional treatment methods. The findings also underscore the need for expanded monitoring networks to track water quality trends over time and assess the effectiveness of intervention measures. Ultimately, the groundwater quality issues identified in Ute Community reflect broader challenges facing many rural and peri-urban areas in developing regions, where rapid environmental change outpaces the development of water management infrastructure. By addressing both the technical and social dimensions of water contamination, and by integrating local knowledge with scientific expertise, sustainable solutions can be developed to safeguard this vital resource. The data presented here provide a foundation for evidence-based decision making and underscore the urgent need for action to protect public health while preserving groundwater resources for future generations. This study contributes to the growing body of knowledge on groundwater quality in Nigeria and offers specific insights that can inform policy development and community action in similar hydrogeological settings across West Africa.

Conflicts of Interest: All authors declare that they have no conflict of interest associated with this research work.
Funding: No special funding was received for this research work.

REFERENCES

1. Adane, T., Adugna, A. T., & Alemayehu, E. (2021). Textile Industry Effluent Treatment Techniques. Journal of Chemistry, 2021. https://doi.org/10.1155/2021/5314404
2. Al-ghouti, M. A., & Da, D. A. (2020). Guidelines for the use and interpretation of adsorption isotherm models: A review. Journal of Hazardous Materials, 393(January), 122383. https://doi.org/10.1016/j.jhazmat.2020.122383
3. Al-Kdasi, A., Idris, A., Saed, K., & Guan, C. T. (2004). Treatment of textile wastewater by advanced oxidation processes– A review. Global Nest Journal, 6(1), 222–230.
4. Aykut-Senel, B., Kaplan-Bekaroglu, S. S., & Ates, N. (2022). Preparation and Characterization of Sulfonic Acid Functionalized Activated Carbon for Applications in Water and Wastewater Treatment. World Congress on Civil, Structural, and Environmental Engineering, 1–7. https://doi.org/10.11159/iceptp22.201
5. Baffour-Awuah, E., Akinlabi, S. A., Jen, T. C., Hassan, S., Okokpujie, I. P., & Ishola, F. (2021). Characteristics of Palm Kernel Shell and Palm Kernel Shell-Polymer Composites: A Review. IOP Conference Series: Materials Science and Engineering, 1107(1), 012090. https://doi.org/10.1088/1757-899x/1107/1/012090
6. Castillo, M., & Barceló, D. (2001). Characterisation of organic pollutants in textile wastewaters and landfill leachate by using toxicity-based fractionation methods followed by liquid and gas chromatography coupled to mass spectrometric detection. Analytica Chimica Acta, 426(2), 253–264. https://doi.org/10.1016/S0003-2670(00)00828-X
7. Gunarathne, V., Ashiq, A., & Ginige, M. P. (2018). Green Adsorbents for Pollutant Removal (Vol. 18, Issue June 2018). https://doi.org/10.1007/978-3-319-92111-2
8. Hamad, H. N., & Idrus, S. (2022). Recent Developments in the Application of Bio-Waste-Derived Adsorbents for the Removal of Methylene Blue from Wastewater: A Review. Polymers, 14(4). https://doi.org/10.3390/polym14040783
9. Jawad, A. H., Ismail, K., Ishak, M. A. M., & Wilson, L. D. (2019). Conversion of Malaysian low-rank coal to mesoporous activated carbon: Structure characterization and adsorption properties. Chinese Journal of Chemical Engineering, 27(7), 1716–1727. https://doi.org/10.1016/j.cjche.2018.12.006
10. Kishor, R., Purchase, D., Saratale, G. D., Saratale, R. G., Ferreira, L. F. R., Bilal, M., Chandra, R., & Bharagava, R. N. (2021). Ecotoxicological and health concerns of persistent coloring pollutants of textile industry wastewater and treatment approaches for environmental safety. Journal of Environmental Chemical Engineering, 9(2). https://doi.org/10.1016/j.jece.2020.105012
11. Madhav, S., Ahamad, A., Singh, P., & Mishra, P. K. (2018). A review of textile industry: Wet processing, environmental impacts, and effluent treatment methods. Environmental Quality Management, 27(3), 31–41. https://doi.org/10.1002/tqem.21538
12. Paredes-Laverde, M., Salamanca, M., Diaz-Corrales, J. D., Flórez, E., Silva-Agredo, J., & Torres-Palma, R. A. (2021). Understanding the removal of an anionic dye in textile wastewaters by adsorption on ZnCl2activated carbons from rice and coffee husk wastes: A combined experimental and theoretical study. Journal of Environmental Chemical Engineering, 9(4). https://doi.org/10.1016/j.jece.2021.105685
13. Pathirana, M. A., Dissanayake, N. S. L., Wanasekara, N. D., Mahltig, B., & Nandasiri, G. K. (2023). Chitosan-Graphene Oxide Dip-Coated Polyacrylonitrile-Ethylenediamine Electrospun Nanofiber Membrane for Removal of the Dye Stuffs Methylene Blue and Congo Red. Nanomaterials, 13(3). https://doi.org/10.3390/nano13030498
14. Pattnaik, P., Dangayach, G. S., & Bhardwaj, A. K. (2018). A review on the sustainability of textile industries wastewater with and without treatment methodologies. Reviews on Environmental Health, 33(2), 163–203. https://doi.org/10.1515/reveh-2018-0013

15. Rashid, R., Shafiq, I., Akhter, P., Iqbal, M. J., & Hussain, M. (2021). A state-of-the-art review on wastewater treatment techniques: the effectiveness of adsorption method. Environmental Science and Pollution Research, 28(8), 9050–9066. https://doi.org/10.1007/s11356-021-12395-x
16. Sabzehmeidani, M. M., Mahnaee, S., Ghaedi, M., Heidari, H., & Roy, V. A. L. (2021). Carbon based materials: A review of adsorbents for inorganic and organic compounds. Materials Advances, 2(2), 598–627. https://doi.org/10.1039/d0ma00087f
17. Sarkar Phyllis, A. K., Tortora, G., & Johnson, I. (2022). Photodegradation. The Fairchild Books Dictionary of Textiles. https://doi.org/10.5040/9781501365072.12105
18. Silva, T. L., Cazetta, A. L., Souza, P. S. C., Zhang, T., Asefa, T., & Almeida, V. C. (2018). Mesoporous activated carbon fibers synthesized from denim fabric waste: Efficient adsorbents for removal of textile dye from aqueous solutions. Journal of Cleaner Production, 171, 482–490. https://doi.org/10.1016/j.jclepro.2017.10.034
19. Velusamy, S., Roy, A., Sundaram, S., & Kumar Mallick, T. (2021). A Review on Heavy Metal Ions and Containing Dyes Removal Through Graphene Oxide-Based Adsorption Strategies for Textile Wastewater Treatment. Chemical Record, 21(7), 1570–1610. https://doi.org/10.1002/tcr.202000153
20. Weber, W. J., & van Vliet, B. M. (1981). Synthetic Adsorbents and Activated Carbons for Water Treatment: Overview and Experimental Comparisons. Journal / American Water Works Association, 73(8), 420–426. https://doi.org/10.1002/j.1551-8833.1981.tb04752.x.